



HAL
open science

Cetylpyridinium removal using phosphate-assisted electrocoagulation, electroreduction and adsorption on electrogenerated sorbents

Abdenacer Flilissa, Philippe Méléard, André Darchen

► **To cite this version:**

Abdenacer Flilissa, Philippe Méléard, André Darchen. Cetylpyridinium removal using phosphate-assisted electrocoagulation, electroreduction and adsorption on electrogenerated sorbents. *Chemical Engineering Journal*, 2016, 284, pp.823-830. 10.1016/j.cej.2015.08.135 . hal-01198730

HAL Id: hal-01198730

<https://univ-rennes.hal.science/hal-01198730>

Submitted on 3 Dec 2015

HAL is a multi-disciplinary open access archive for the deposit and dissemination of scientific research documents, whether they are published or not. The documents may come from teaching and research institutions in France or abroad, or from public or private research centers.

L'archive ouverte pluridisciplinaire **HAL**, est destinée au dépôt et à la diffusion de documents scientifiques de niveau recherche, publiés ou non, émanant des établissements d'enseignement et de recherche français ou étrangers, des laboratoires publics ou privés.

**Cetylpyridinium removal using phosphate-assisted electrocoagulation,
electroreduction and adsorption on electrogenerated sorbents**

Abdenacer Flilissa¹, Philippe Méléard, André Darchen*

UMR CNRS n°6226 Institut des Sciences Chimiques de Rennes, ENSCR, CS 50837, 35708

Rennes Cedex 7, France

* Corresponding author: Tel.: +33 223238004. Fax: +33 223238199.

E-mail address: Andre.Darchen@ensc-rennes.fr (A. Darchen)

¹ Present address: *Laboratoire de Chimie Analytique, Département de Pharmacie, Faculté de Médecine, Université Ferhat Abbas, Sétif 1, 19000 Algeria*

Abstract

Cetylpyridinium (CP^+) is a cationic surfactant that can be found in various effluents and known due its toxicity against aquatic organisms. The removal of this compound was investigated in water solutions by electrocoagulation, phosphate-assisted electrocoagulation and adsorption on electrogenerated adsorbents. Electrocoagulations were carried out with aluminum electrodes in CP^+ synthetic solutions. After 2 h of electrolysis in 0.1 M NaCl solutions, CP^+ was mainly removed by electroreduction at calculated rates of 0.024 and 0.0416 $\mu\text{mol}/\text{C}$ corresponding to abatements of 28 and 24% for starting concentrations of CP^+ at 0.5 mM and 1.0 mM, respectively. The voltammetric study on steel or graphite electrodes confirmed a possible electroreduction of CP^+ which may explain its removal during electrolysis. The change of the cathode from aluminum to carbon or steel did not change notably the removal efficiency of electrolysis in 0.1 M NaCl solution. However, after 2 h of electrolysis in 0.1 M NaCl in the presence of 0.1 M phosphate buffer, CP^+ was mainly removed by adsorption on electrogenerated aluminum phosphate with rates of 0.0694 and 0.138 $\mu\text{mol}/\text{C}$ corresponding to abatements of 80% for 0.5 or 1 mM CP^+ solutions. The key role of phosphate ions was proved by adsorption experiments. The electro-synthesized alumina adsorbed CP^+ with a removal capacity of 10.2 mg/g. But on electro-synthesized and chemical-synthesized aluminum phosphate the removal capacities were 94.2 and 165.3 mg/g, respectively.

Key-words: Aluminum phosphate; Surfactants; Electrolysis; Alumina; Adsorption; Reduction

1. Introduction

The increasing consumption of water and high-quality water drives the development of efficient water treatments and the research of new processes which are able to remove emerging pollutants [1]. Among these pollutants, surfactants constitute a large class of chemical substances that are widely used in domestic and industrial processes thanks to their physicochemical characteristics such as detergency, foaming, emulsification and dispersion effects. Surfactants are involved in various environmental pollutions with toxic effect on living organisms [2] and have raised problems in wastewater treatment plants [3]. Therefore, the removal of surfactants from wastewater is important in reducing their environmental impact. Classical techniques like oxidation, adsorption extraction or coagulation have been used. In this context electrochemical treatments and specially electrocoagulation (EC) have been applied in the removal of few surfactants [4,5].

EC is a well-known electrochemical treatment which uses soluble anode materials in order to generate metal ions involved in a coagulation step [6,7]. According to Holt et al. [6] EC is a combination of physico-chemical processes including electrochemistry, coagulation and flotation. EC is efficient in the treatment of a large variety of effluents [8]. It is often emphasized that chemicals are not required in EC when it is directly applied to a wastewater. This is not strictly true because sacrificial anodes are consumed in all cases, and sometimes an efficient treatment needs a pH control and the addition of an electrolyte [9]. Generally, it is considered that the electrolyte is not consumed during EC, but it can play a key role in the efficiency of the treatment [10] or in the structure of the electro-generated alumina [11]

Some pollutants are resistant to EC. This is the case with targeted compounds which are not involved in an electrochemical reaction or when they are not adsorbed on electro-generated alumina. To overcome these difficulties, a new class of EC appears where chemicals are used as assistance in the process. Addition of ozone [12], hydrogen peroxide [13] or a chemical coagulant improves the corresponding assisted electrocoagulation.

In this paper we present a new example of a chemical-assisted EC applied to the removal of N-cetylpyridium cation (CP^+) from synthetic solutions. CP^+ is a cationic surfactant which exhibits toxicity against aquatic organisms [14]. The extensive use of CP^+ has led to the investigation of its removal from water solutions. Main methods use adsorption onto high-area activated carbon [15], or granular charcoal [16]. Photo-catalytic oxidation over TiO_2 photo-catalyst [17] has also been investigated. In the present paper, the removal of CP^+ is

investigated in classical EC and in a more efficient phosphate-enhanced EC. Reduction and adsorption on electrogenerated alumina, phosphate modified alumina and aluminum phosphate are removal ways of CP⁺.

2. Materials and methods

2.1. Chemicals

CP⁺ solutions were prepared with N-cetylpyridinium bromide (C₂₁H₃₈NBr 98%) from Aldrich. Sodium dihydrogen phosphate dihydrate (NaH₂PO₄·2H₂O 99%) and disodium hydrogen phosphate (Na₂HPO₄ 99%) were Prolabo analytical reagents. Sodium nitrate (NaNO₃, 99%), hydrochloric acid (HCl 36%), and sodium hydroxide (NaOH 99%) were Fluka reagents. Aluminum chloride hexahydrate (AlCl₃·6H₂O, Prolabo 99%) was used in the preparation of alumina and aluminum phosphate adsorbents. Phosphoric acid (H₃PO₄, 85%), nitric acid (HNO₃, 65%), sodium chloride (NaCl 99%), sulfuric acid (H₂SO₄ 96%), iron powder (97%), zinc powder (97%) and aluminum powder (99%) were Fluka reagents. All aqueous solutions were prepared by dissolution in de-ionized water.

2.2. Electrolysis

CP⁺ removal by EC was investigated in 0.1 M NaCl or in 0.1 M NaCl buffered by 0.1 M Na₂HPO₄ and 0.1 M NaH₂PO₄. All the electrolyses were conducted at 0.2 A on 0.25 L of solution with aluminum electrodes with a surface of 15 cm² (width 3 cm, 5 cm length). The gap between anode and cathode was 1.8 cm. Solutions were magnetically stirred. Three or five cells were connected on series. One of these cells was used as a control. Before electrolysis the electrodes were immersed in 2 M NaOH solution for 2 min and then rinsed with de-ionized water, dried in an oven and finally weighed. The electrolysis current was supplied by a current generator (Microlab 300V-1A). During electrolysis, pH was measured with a pH meter (Metrohm 827) and a combined glass electrode. A turbidimeter (Hach 2100P) was used to measure turbidity. The conductivity was measured with a conductimeter (CDM MeterLab 210) and a conductivity cell (E61M013). In order to maintain a constant volume during the electrolyses the analyzed solutions were put back in the electrolytic cells. At the end of electrolysis, the electrolytic solution was filtered and the recovered solid was

washed, oven dried at 105°C, and finally weighed. Electrodes were weighed at the end of electrolysis. Steel and graphite cathodes which were used in electrolysis were of identical dimensions to those of the aluminum cathode.

2.3. Voltammetric study

The voltammetric behavior of 0.02 M CP⁺ was investigated in 0.1 M NaCl solution at 22°C. Solutions were deoxygenated by bubbling nitrogen for 15 min. The working electrode was a micro-disk of glassy carbon of 4 mm diameter. The auxiliary electrode and the reference electrode were a rod of glassy carbon and a saturated calomel electrode (SCE), respectively. A potentiostat EG*G model 362 and a XY recorder were used in the recording of voltammograms.

2.4. Aluminophosphate and phosphate-modified alumina

Two kinds of aluminophosphate were prepared by electrolysis and chemical precipitation. In the discussion, they are designated by (AlPO₄)_E and (AlPO₄)_C. (AlPO₄)_E was prepared by electrolysis at 0.2 A for 10 h with aluminum electrodes in 0.25 L of a buffer solution 0.1 M Na₂HPO₄ and 0.1 M NaH₂PO₄ in the presence of 0.1 M NaCl. (AlPO₄)_C was obtained by precipitation after addition of Na₃PO₄ solution to a solution of AlCl₃. Phosphate modified alumina was prepared by adsorption of phosphate onto alumina. In a first time, alumina was prepared by electrolysis at 0.2 A for 10 h with aluminum electrodes in 0.25 L of 0.1 M NaCl solution. Then 0.2 g of the isolated alumina was stirred for 2 h in 50 mL of a 4 mM NaH₂PO₄ solution. The solid isolated was oven dried at 105°C.

2.5. Determination of pH at the point of zero charge (pH_{pzc})

The point of zero charge (PZC) of all solids was estimated by using the batch equilibrium technique [18]. In this purpose, 0.2 g of solid was treated with 50 mL of 0.1 M NaNO₃ solution which was used as an inert electrolyte. The initial pH (pH_i) was adjusted in the range 3–11 by addition of 0.01 M NaOH or 0.01 M HNO₃. The suspensions were left for 24 h to reach their thermodynamic equilibrium on a rotary shaker operating at 350 rpm. After

completion of the equilibrium time, the solutions were filtered and the final pH (pH_f) of the filtrates was measured.

2.6. Analysis

UV-Vis spectrophotometer (Perkin Elmer Lambda 35) was used in quantitative analysis of CP⁺ in solutions at $\lambda_{\text{max}} = 259$ nm and an infrared spectrophotometer (FTIR - Shimadzu) in analysis of the adsorbents. The specific area of adsorbents was determined by the BET method. The instrument used was a model AS1 KR/MP version 5.52 using a software version 2.01 and a stand-conditioning sample Micromeritics Flow Prep 060, set at a temperature between 140°C and 145°C.

2.7. Adsorption kinetic

In each experiment, 50 mL of CP⁺ solutions at 0.3 mM, 0.5 mM, 0.7 mM or 0.9 mM were stirred at 250 rpm with 0.2 g of adsorbent at $22 \pm 1^\circ\text{C}$. Samples were withdrawn at appropriate time intervals and centrifuged at 4000 rpm for 10 min. The CP⁺ absorbance of the supernatant solution was measured. The initial pH value was maintained higher than the pH_{pzc} by addition of few drops of a concentrated NaOH solution. The CP⁺ uptake by adsorbents was calculated by Eq. (1) where q_t (mmol/g) is the amount of adsorbed CP⁺ at time t (min), V (L) is the volume of solution, C_0 and C_t (mmol/L) are concentrations at initial and time t , respectively and m (g) is the mass of adsorbent.

$$q_t = (C_0 - C_t) V/m \quad (1)$$

2.8. Adsorption isotherm

The isotherm studies were carried out using a range of initial CP⁺ concentrations of 0.3 to 2.5 mM. A typical experiment was conducted in a batch process by adding 0.2 g of the adsorbent to 50 mL of CP⁺ solution. The mixture was stirred at 250 rpm for 3 and 6 h in the presence of adsorbents (AlPO₄)_C and (AlPO₄)_E, respectively. The mixture was centrifuged at 4000 rpm for 10 min and the residual CP⁺ concentration was determined in the supernatant solution. The amount of adsorbed CP⁺ at equilibrium q_e (mmol/g) was obtained by Eq. (2) where C_0 and C_e (mmol/L) are initial concentration and equilibrium concentration of CP⁺, respectively, V (L) is the volume of solution, and m (g) is the mass of adsorbent.

$$q_e = (C_0 - C_e) V/m \quad (2)$$

3. Results and discussions

3.1. Electrocoagulation in NaCl solution

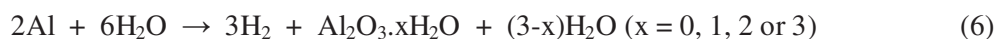
The electrolysis of CP^+ was performed at 22°C in 0.1 M NaCl solution. The electrolysis current was controlled at 0.2 A in order to prevent an excessive foam formation. After 570 min of electrolysis, the mass loss of the anode was 0.77 g whereas the calculated value according to Faraday's law was 0.637 g. The cathode showed also a mass loss of 0.28 g due to a cathodic corrosion. These mass losses of aluminum anode and cathode are classical observations during EC [19]. A mass of 2.6 g of the electrogenerated alumina was isolated at the end of the electrolysis.

Owing to the formation of alumina, the turbidity of the aqueous medium increased. Remarkably, as shown by results in Fig. 1, the turbidity increased with increasing CP^+ concentration from 4 to 16 mM CP^+ . This observation shows that CP^+ is involved in the coagulation process. A correct explanation of that increased turbidity would require more experiments.

The pH increased at the beginning of electrolysis and reached an approximate constant value (Fig. 2). The greatest pH value shows a noteworthy decrease when the CP^+ concentration increases. Without CP^+ the pH reaches 9, whereas in solutions of 4 mM, 8 mM and 16 mM CP^+ the pH increases until 8.4, 8.0 and 7.5, respectively. An increase of the pH is frequently observed during EC in NaCl solution. It is explained by a partial formation of $Al(OH)_2Cl$ instead of the expected $Al(OH)_3$ [11]. As explained below, the effect of CP^+ concentration on the particular pH variation reveals the involvement of the reduction of CP^+ during this EC.

In the absence of CP^+ in NaCl solution, the EC process can be described by Eqs. (3)-(6). The anodic reaction (Eq. (3)) leads to the formation of Al^{3+} ions. The cathodic reduction of water (Eq. (4)) produces hydrogen and hydroxyl anion. Al^{3+} and OH^- ions react to form alumina following Eq. (5). The structure of alumina depends upon the water content of $Al_2O_3 \cdot xH_2O$. In most cases, X-ray diffraction of the isolated electrogenerated alumina shows that $AlOOH$ is the main compound obtained beside $Al(OH)_3$ [11]. The overall reaction is summarized by Eq. (6). This only reaction does not account for the observed increase of pH

which is explained by the concomitant reaction (Eq. (7)) where a chloride anion is involved in an anion exchange with the release of one hydroxyl anion [11].



In the presence of CP^{+} , a coupling cathodic reduction happened following Eq. (8). The involvement of this reduction increased with the concentration of CP^{+} . The consequence was a competition between two cathodic reactions (Eqs. (4) and (8)) and a decrease in the formation of hydroxyl anions and a lower pH increase as observed (Fig. 2).



The CP^{+} abatement observed after 570 min of electrolysis at CP^{+} concentrations of 4 mM, 8 mM and 16 mM were 55%, 49% and 61%, respectively. At 4 mM CP^{+} the amount of CP^{+} adsorbed on 2.6 g of electrogenerated alumina was 0.104 mmol (see later in section 3.4.2). Assuming that the same amount of CP^{+} (0.104 mmol) was adsorbed during EC, the abatement of CP^{+} due to reduction during EC is calculated to be about 44.6% at initial 4 mM CP^{+} . The IR spectrum of the solid isolated after electrolysis of 4 mM CP^{+} was in agreement with the presence of adsorbed surfactant and the dimer $(\text{CP})_2$. The bands which were observed at 2930 and 2863 cm^{-1} were attributed to the stretching of CH_2 in the cetyl group [20]. These stretching vibrations do not allow a distinction between CP^{+} and its reduction product.

Fig. 1.

Fig. 2.

In order to minimize the reduction of CP^{+} , electrolyses were realized with initial CP^{+} concentrations of 0.5 mM and 1 mM (amount of 0.125 mmol and 0.25 mmol of CP^{+} in 0.25 L). The variations of CP^{+} concentration versus electrolysis time are represented in Fig. 3. After 810 min of electrolysis, an almost complete removal of CP^{+} was observed and 3.2 g of alumina were isolated. The alumina amount allowed a 95% CP^{+} removal involving

adsorption. At initial CP^+ concentration of 1 mM, the observed yield of CP^+ removal was 2.44×10^{-5} mmol/C or 0.078 mmol/g of electrogenerated alumina, or 2.35 mmol of CP^+ /mol of electrons.

Fig. 3.

3.2. Reduction of CP^+

This investigation was carried out in order to prove the reduction of CP^+ during EC experiments and to find if this reaction would be an efficient electrochemical treatment. The possibility of a reduction during EC is not surprising since the involvement of reduction is well known during the removal of nitrate anions [21] and pyridinium cations are known as reducible substrates on various electrode materials [22].

3.2.1. Voltammetry of CP^+

The voltammetric study was performed in 0.1 M NaCl solution at a working electrode of glassy carbon. The voltammograms show a one-electron irreversible cathodic peak at -1.05 V/SCE and one irreversible anodic peak at -0.02 V/SCE (Fig. 4). Both peaks increase with the CP^+ concentration. The cathodic peak current is proportional to the CP^+ concentration. The one-electron reduction leads to a neutral radical which undergoes a fast dimerization. The anodic peak is rather symmetric in agreement with the oxidation of adsorbed species. The anodic peak was observed only after the cathodic one proving that the oxidation must be attributed to the oxidation of the reduced compound which was formed during the cathodic potential scan. The voltammetric behavior of CP^+ is summarized in Fig. 5, assuming that the dimer is the 4,4' coupled isomer. During the anodic potential scan, the dimer is oxidized leading to the starting substrate. Owing to this chemical reversibility, repetitive potential scans did not show a current decrease. The potential of the electrochemical reduction was constant in the pH range 1-13, as expected when a process does not involve protonation. This electrochemical behavior is analogous to the one of N-alkylpyridinium cations [22].

Fig. 4.

Fig. 5.

3.2.2. Effect of the cathode during EC

In order to check the behavior of CP^+ and its abatement during EC different cathodes were used. Electrolyses were carried out in 0.1 M NaCl solution with aluminum anode and steel or graphite cathodes. Electrolyses were carried out for 0.5 and 1 mM CP^+ under a current of 0.2 A. Fig. 6 shows the decrease of the CP^+ concentration as a function of electrolysis time. The abatements of CP^+ seem similar to what is observed with an aluminum cathode. After 570 min of electrolysis, abatements reached 59% and 68% at CP^+ initial concentrations of 1 mM, when cathodes were steel and graphite, respectively. An abatement of 67% was observed after 570 min of electrolysis when an aluminum cathode was used (Fig. 3).

Fig. 6.

3.2.3. Reduction of CP^+ by metal powder

The chemical reduction of CP^+ was investigated in order to confirm its possible removal by reduction. Aluminum, zinc and iron were used at pH 13.3, 1.2 and 1.5, respectively, in order to prevent the passivity of these reducing metals. The apparent standard potentials of Al and Zn at pH 13.3 and 1.2 are -2.31 V/SHE and -0.76 V/SHE, respectively. These metals are able to reduce CP^+ which shows a cathodic peak at -0.80 V/SHE, taking the potential of the SCE at $+0.246$ V/SHE. The treatment of 1 mM CP^+ solutions by stoichiometric quantities of Al and Zn powder afforded a 90% abatement of CP^+ . As expected by the low standard potential of iron at -0.44 V/SHE, iron powder did not reduce CP^+ .

3.3. EC in the presence of phosphate ions

EC was carried out in the presence of phosphate ions in order to modify the structure of the electrogenerated adsorbent. It is well known that EC is efficient in the removal of phosphate [23] and this is in agreement with the formation of insoluble aluminophosphate. EC was performed at 0.2 A for 420 min in 0.1 M NaCl solution buffered by 0.1 M Na_2HPO_4 and 0.1 M NaH_2PO_4 . At the end of the electrolysis, the experimental mass losses of aluminum anodes and cathodes were 0.550 g and 0.12 g, respectively. The mass loss due to corrosion of both electrodes is calculated at 0.2 g.

Fig. 7 shows the variation of pH during electrolysis in the presence or without CP^+ . For the first 3 h, the pH increased slowly from 6.4 to 7.0, in agreement with a buffer effect of phosphate compounds. Then, for the 4th hour, the pH increase was faster and reached 9.6.

These pH variations contrast with the results of Fig. 2 and look like the titration curve of an acid by a base showing a pseudo equivalent point at about 250 min. Analogous pH variation has been already observed during EC of H_3PO_4 solutions [24]. In this case, the equivalence point corresponds to the total transformation of phosphoric acid into aluminum phosphate. In the case of Fig. 7, the interpretation is slightly different. Considering the formation of AlPO_4 by reaction of Al^{3+} following Eq. (9). The combination of Eqs. (3), (4), (9) and (10) gives the overall reaction (Eq. (11)) which shows that one mole of Al^{3+} arising from anode dissolution consumes 2 moles of H_2PO_4^- . Considering the formation of alumina by aluminum corrosion (Eq. (12)) where alumina is written $\text{Al}(\text{OH})_3$ in order to simplify. The involvement of Eqs. (10) and (12) in the formation of AlPO_4 (Eq. (13)) gives the overall Eq. (14) which is identical to Eq. (11). This relation also shows that one mole of $\text{Al}(\text{OH})_3$ arising from Al corrosion consumes 2 moles of H_2PO_4^- and gives one mole of the basic specie HPO_4^{2-} which is involved in the pH increase.



Fig. 7.

From the mass loss of electrodes at the end of electrolysis, the amount of Al which was corroded at the pseudo-equivalence of 250 min was calculated at 0.119 g corresponding to the possible formation of 4.41 mmol of $\text{Al}(\text{OH})_3$. At the same time, the quantity of Al^{3+} was 10.36 mmol according to Faraday's law. Al^{3+} and $\text{Al}(\text{OH})_3$ allow the disappearance of 29.54 mmol of H_2PO_4^- and 250 mL of the 0.1 M H_2PO_4^- solution contained 25 mmol of H_2PO_4^- . So, the pseudo-equivalence observed at 250 min is not in a very good agreement with the formation of an aluminophosphate written as AlPO_4 in this paper. The difference between the calculated and the observed values may be attributed to a difference between the real structure of the aluminophosphate and AlPO_4 .

The variation of CP^+ concentration during EC in the presence of a phosphate buffer is given in Fig. 8. At the end of electrolyses, a mass of 3.37 g of dried aluminophosphate was

isolated. The CP^+ abatement shown in Fig. 8 is at 95% after 3 h of electrolysis. The abatement can be calculated at this time at initial CP^+ concentration of 1 mM. It was 0.164 mmol/g of electrogenerated $AlPO_4$ or $10.97 \cdot 10^{-5}$ mmol/C or 10.59 mmol/mol of electrons. In the presence of a phosphate buffer, the CP^+ removal during EC was 4.5 times more efficient than in the absence of this buffer.

Fig. 8.

3.4. Adsorption

3.4.1. Structure of the investigated adsorbents

The structure of the alumina electrogenerated in NaCl solutions is already described as a mixture of boehmite $AlOOH$ and bayerite $Al(OH)_3$ [5,11]. The XRD of $(AlPO_4)_C$ and $(AlPO_4)_E$ showed an amorphous structure. The phosphate-modified alumina was prepared by immersion of an electrogenerated alumina into a 4 mM NaH_2PO_4 solution. During this immersion the alumina surface was modified thanks to an efficient phosphate adsorption [23]. The analysis of P by EDS gave a weight content of 1.54%. The specific surface area of solids were determined by BET method and gave 100 and 27 m^2/g for $(AlPO_4)_C$ and $(AlPO_4)_E$, respectively, and 217 m^2/g for alumina arising from EC in 0.1 M NaCl. The large difference between BET surface areas of $(AlPO_4)_C$ and $(AlPO_4)_E$ probably arises from the kinetics of the synthesis ways. The chemical synthesis is faster than the electrochemical one and this allows the formation of a higher surface. The pH_{pzc} of $(AlPO_4)_C$ and $(AlPO_4)_E$ were respectively 4.75, 7.55 and the pH_{pzc} of the electrogenerated alumina was 8.1.

3.4.2. Adsorption of CP^+ on electrogenerated adsorbents

In order to verify the removal of CP^+ by adsorption, electrolyses were carried out in 0.1 M NaCl and in the absence of CP^+ for 570 min. The experimental mass loss of both electrodes was 1.0 g including the mass loss of cathode by corrosion. At the end of electrolyses, CP^+ was added at the concentrations of 2 and 4 mM and its concentration was measured. After 2 h of stirring, at initial concentration of 4 mM, the results showed that the rate of CP^+ removal was calculated to be 0.04 mmol/g. This CP^+ adsorption on 2.6 g of electrogenerated alumina corresponds to 1.47 mmol/mol of electrons. This result shows that EC was more efficient than adsorption in the removing of CP^+ .

Electrolyses were carried out in 0.1 M NaCl buffered with phosphate buffer without surfactant. After 420 min of electrolysis, 3.2 g of an oven dried solid of aluminophosphate were isolated. They were added to a cell that contained 0.25 L of 1 mM CP⁺. The mixture was magnetically stirred and the change in concentration of CP⁺ was observed. The results showed a 97% decrease of CP⁺ after 2 h corresponding to 0.076 mmol/g of AlPO₄ or 4.82 10⁻⁵ mmol/C or 4.65 mmol/mol of electrons. In this experiment, the adsorption on electrogenerated AlPO₄ is 3.16 times more efficient than adsorption on electrogenerated alumina. The result also shows that EC in the presence of a phosphate buffer was more efficient than adsorption on electrogenerated AlPO₄ in removing CP⁺.

The IR spectra of the isolated solids were in agreement with the presence of adsorbed CP⁺ as shown by the vibration bands at 2925 and 2853cm⁻¹ which were attributed to the stretching of -CH₂- of the cetyl group.

3.4.3. Adsorption kinetics of CP⁺ on aluminophosphate

Various models are available to study the kinetics of adsorption. Two models were used in the adsorption of CP⁺ onto (AlPO₄)_E and (AlPO₄)_C: the pseudo-first-order and the pseudo-second-order. The Lagergren rate equation is one of the most widely used rate relation to describe the adsorption process. The pseudo-first-order equation is given by Eq. (15) [25], whereas the pseudo-second-order model is rather governed by Eq. (16) as described in the literature [26] where q_e (mmol/g) and q_t (mmol/g) are the amounts of CP⁺ adsorbed at equilibrium and at time t, respectively, k₁ (min⁻¹) and k₂ (g/mmol min) are rate constants of the first order and the second order, respectively.

$$\log (q_e - q_t) = \log q_e - k_1 t / 2.303 \quad (15)$$

$$t / q_t = 1 / k_2 q_e^2 + t / q_e \quad (16)$$

The experimental study of the adsorption kinetics of CP⁺ on (AlPO₄)_C (Fig. 9a1) showed a fast adsorption in the first minutes and reached a steady state, particularly at concentrations below the Critical Micelle Concentration (CMC). The CMC of CP⁺ bromide in water at 25°C is of 0.7 mmol/L [27]. The CMC of CP⁺ bromide in 0.1 M NaCl solution was determined by UV-Vis and was found to be 0.016 mmol/L.

The linear relations (Eqs. (15) and (16)) were used in the investigation of the adsorption process. For the first order, log(q_e - q_t) was plotted versus t. The values of k₁ were

calculated from the slope of the linear plots. For the second order, t/q_t was plotted versus t . The values of q_e were obtained from $1/\text{slope}$, and from intercept $(1/k_2q_e^2)$ k_2 can be calculated. The correlations coefficient values R^2 showed that the pseudo-second-order model gave a better fit than the pseudo-first-order model. The coefficients R^2 are in the ranges 0.9994 - 0.9804 and 1 - 0.9999 for $(\text{AlPO}_4)_E$, and $(\text{AlPO}_4)_C$ respectively (Table 1). These values are significantly higher than those obtained with a pseudo-first-order model. Results for the second order are gathered in Table 1: The rate constant decreases from 0.9205 to 0.0693 g/mmol min and 16.63 to 1.555 g/mmol min, for $(\text{AlPO}_4)_E$, and $(\text{AlPO}_4)_C$, respectively when the initial surfactant concentration increases from 0.3 mM to 0.9 mM. q_e increases with the initial concentration of CP^+ . Experimental values of q_e are very close to calculated values (Table1).

The kinetics of adsorption of CP^+ on $(\text{AlPO}_4)_E$ (Fig. 9b1) was slower than on $(\text{AlPO}_4)_C$ and its adsorption capacity at equilibrium was lower than the one found for $(\text{AlPO}_4)_C$.

Table 1.

3.4.4. Adsorption isotherms of CP^+ on aluminophosphate

For a solid-liquid system, the equilibrium of adsorption is one of the important physico-chemical aspects in the description of adsorption behavior.

The adsorption isotherm of CP^+ on $(\text{AlPO}_4)_C$ shows a maximum adsorption capacity of 0.43 mmol/g (165.3 mg/g) (Fig. 9a2). The initial CP^+ concentrations were chosen higher than its CMC ($C_e > \text{CMC}$). At these concentrations the adsorption onto $(\text{AlPO}_4)_C$ increases and the CP^+ is associated with the adsorbent by lateral interactions between the hydrocarbon chains. CP^+ was assumed to be adsorbed as hemimicelles and by the formation of admicelles between 0.02 and 0.2 mM [28] and hemimicelles - admicelles between 0.2 and 0.3 mM [29]. The isotherm at concentrations $C_e > \text{CMC}$ is of type III. It corresponds to a solid non-porous or porous which is characterized by weak interactions adsorbate/adsorbent.

The rate of adsorption of CP^+ on $(\text{AlPO}_4)_E$ is slower than that obtained on $(\text{AlPO}_4)_C$ especially at concentrations above the CMC (Fig. 9b2). The isotherm shows the greatest adsorption capacity at 0.245 mmol/g (94.19 mg/g). The results between 0.08 and 0.25 mM show a fast formation of admicelle [30] and the formation of hemimicelles - admicelle [29]. The isotherm at concentrations $C_e > \text{CMC}$ is of type III.

Fig. 9.

3.4.5. Adsorption kinetics and isotherm of CP^+ on phosphate-modified alumina

The variation in the adsorption capacity of CP^+ as a function of pH on an alumina modified by adsorbed phosphate showed a maximum adsorption capacity of 0.06 mmol/g at pH 6.9. The adsorption study was performed with 0.3 mM and 1 mM CP^+ concentrations. The adsorption rate was slower than to the one obtained on $(AlPO_4)_C$ but equivalent to the rate of adsorption on $(AlPO_4)_E$. The results are shown in Fig. 10a.

The application of pseudo-first-order and pseudo-second-order models in the adsorption kinetics gives a better fit with the pseudo-second-order model with R^2 values greater than 0.99. XRD diagrams of the modified and unmodified alumina showed a slight difference which may be attributed to the presence of adsorbed phosphate on the surface of the alumina. The adsorption isotherm of the modified alumina CP^+ has an adsorption capacity of 0.275 mmol/g (Fig. 10b).

Fig. 10.

3.4.7. Comparison of the investigated adsorbents

Three kinds of adsorbents were investigated in this work: two electrogenerated adsorbents: alumina and $(AlPO_4)_E$, one alumina modified by adsorbed phosphate and one chemically synthesized phosphate $(AlPO_4)_C$. The results of adsorption capacity showed that EC was more efficient in CP^+ removal than adsorption on the corresponding electrogenerated adsorbents. The alumina modified by adsorbed phosphate and all $AlPO_4$ were more efficient in CP^+ removal than alumina. The best adsorption capacity was observed on the aluminum phosphate chemically synthesized $(AlPO_4)_C$.

4. Conclusion

For the first time, the removal of CP^+ was investigated by EC using aluminum electrodes. The study revealed that this EC was a complicated process involving electroreduction of CP^+ and adsorption on electrogenerated adsorbents. The efficiency of the CP^+ removal was improved by performing EC in the presence of phosphate ions. The pH variations during EC were informative about two reactions which are involved: (i) the reduction of CP^+ in competition with water reduction and (ii) the formation of aluminophosphate when EC was performed in the presence of phosphate ions. The efficiency

of the CP⁺ removal during EC was confirmed by an adsorption study. Results showed the following order of decreasing adsorption capacity: (AlPO₄)_C > alumina modified by adsorbed phosphate > (AlPO₄)_E > electrogenerated alumina. The CP⁺ removal was more efficient during the EC treatments than by adsorption on the corresponding electrogenerated adsorbents alumina or aluminophosphate.

Acknowledgements

The authors thank CNRS (UMR 6226) and the French Ministry of National Education for positions and support. One of us (A. Fililissa) wishes to express his gratitude to the Ministère de l'Enseignement Supérieur et de la Recherche Scientifique of Algeria for a doctoral fellowship.

References

- [1] M. La Farre, S. Perez, L. Kantiani, D. Barcelo, Fate and toxicity of emerging pollutants, their metabolites and transformation products in aquatic environment, *Trends Anal. Chem.* 27 (2008) 991-1007.
- [2] T. Ivankovic, J. Hrenovic, Surfactants in the environment, *Arch. Ind. Hyg. Toxicol.* 61 (2010) 95-110.
- [3] J. Hrenovic, T. Ivankovic, Toxicity of anionic and cationic surfactant to *Acinetobacter junii* in pure culture, *Cent. Eur. J. Biol.* 2 (2007) 405-414.
- [4] E. Onder, A.S. Kopal, U.B. Ogutveren, An alternative method for the removal of surfactants from water: electrochemical coagulation, *Sep. Purif. Technol.* 52 (2007) 527-532.
- [5] A. Fililissa, A. Darchen, P. Méléard, Selective removal of dodecyl sulfate during electrolysis with aluminum electrodes, *Desalination Water Treat.* 51 (2013) 6719-6728.
- [6] P.K. Holt, G.W. Barton, C.A. Mitchell, The future for electrocoagulation as a localized water treatment technology, *Chemosphere*, 59 (2005) 355-367.
- [7] H. Liu, X. Zhao, J. Qu, Electrocoagulation in water treatment in C. Comninellis, G. Chen (Eds), *Electrochemistry for the Environment* (2010) 245-262.

- [8] I. Kabdasli, I. Arslan-Alaton, T. Olmez-Hanci, O. Tunay, Electrocoagulation applications for industrial wastewaters: a critical review, *Environ. Technol. Rev.* 1 (2012) 2-45.
- [9] M. Mechelhoff, G.H. Kelsall, N.J.D. Graham, Electrochemical behavior of aluminium in electrocoagulation processes, *Chem. Eng. Sci.* 95 (2013) 301-312.
- [10] J.L. Trompette, H. Vergnes, On the crucial influence of some supporting electrolytes during electrocoagulation in the presence of aluminum electrodes, *J. Hazard. Mater.* 163 (2009) 1282–1288.
- [11] E. Tchomgui-Kamga, N. Audebrand, A. Darchen, Effect of co-existing ions during the preparation of alumina by electrolysis with soluble aluminum electrodes: structure and defluoridation activity of electro-synthesized adsorbents, *J. Hazard. Mater.* 254-255 (2013) 125-133.
- [12] S. Song, Z. He, J. Qiu, L. Xu, J. Chen, Ozone assisted electrocoagulation for decolorization of C.I. Reactive Black 5 in aqueous solution: an investigation of the effect of operational parameters, *Sep. Purif. Technol.* 55 (2007) 238-245.
- [13] G. Roa-Morales, E. Campos-Medina, J. Aguilera-Cotero, B. Bilyeu, C. Barrera-Diaz, Aluminum electrocoagulation with peroxide applied to wastewater from pasta and cookie processing, *Sep. Purif. Technol.* 54 (2007) 124-129.
- [14] J. Hrenovic, T. Ivankovic, L. Sekovanic, M. Rozic, Toxicity of dodecylpyridinium and cetylpyridinium chlorides against phosphate-accumulating bacterium, *Cent. Eur. J. Biol.* 3 (2008) 143-148.
- [15] O. Duman, E. Ayranci, Adsorptive removal of cationic surfactants from aqueous solutions onto high-area activated carbon cloth monitored by in situ UV spectroscopy, *J. Hazard. Mater.* 174 (2010) 359–367.
- [16] M.M. Saleh, On the removal of cationic surfactants from dilute streams by granular charcoal, *Water Res.* 40 (2006) 1052–1060.
- [17] B. Singhal, A. Porwal, A. Sharma, R. Ameta, S.C. Ameta, Photocatalytic degradation of cetyl pyridinium chloride over titanium dioxide powder, *J. Photochem. Photobiol A: Chem.* 108 (1997) 85-88.
- [18] F. Gaboriaud, J.J. Ehrhardt, Effect of different crystal faces on the surface charge of colloidal goethite (α -FeOOH) particles: an experimental and modeling study, *Geochimica Cosmochimica Acta* 67 (2003) 967-983.
- [19] M. Mechelhoff, G.H. Kelsall, N.J.D. Graham, Super-faradaic charge yields for aluminium dissolution in neutral aqueous solutions, *Chem. Eng. Sci.* 95 (2013) 353-359.

- [20] K.-H.S. Kung, K.F. Hayes, Fourier transform infrared spectroscopic study of the adsorption of cetyltrimethylammonium bromide and cetylpyridinium chloride on silica, *Langmuir*, 9 (1993) 263-267.
- [21] A.S. Koparal, U.B. Ogutveren, Removal of nitrate from water by electroreduction and electrocoagulation, *J. Hazard. Mater.* 89 (2002) 83-94.
- [22] J.G. Gaudiello, D. Larkin, J.D. Rawn, J.J. Sosnowski, E.E. Bancroft, H.N. Blount, On the mechanism of the electrochemical reduction of N-methylpyridinium ion, *J. Electroanal. Chem.* 131 (1982) 203-214.
- [23] S. Tanada, M. Kabayama, N. Kawasaki, T. Sakiyama, T. Nakamura, M. Araki, T. Tamura, Removal of phosphate by aluminium oxide hydroxide, *J. Colloid Interface Sci.* 257 (2003) 135-140.
- [24] S. Tchamango, C.P. Nanseu-Njiki, E. Ngameni, D. Hadjiev, A. Darchen, Treatment of dairy effluents by electrocoagulation using aluminum electrodes, *Sci. Total Environ.* 408 (2010) 947-952.
- [25] S. Lagergren, Zur theorie der sogenannten adsorption geloster stoffe, *Kungliga Svenska Vetenskapsakademiens. Handlingar* 24 (1898) 1-39.
- [26] Y.S. Ho, Second-order-kinetic model for the sorption of cadmium onto tree fern: a comparison of linear and non-linear methods, *Water Res.* 40 (2006) 119-125.
- [27] J.J. Chung, S.W. Lee, J.H. Choi, Salt effects on the critical micelle concentration and counterion binding of cetylpyridinium bromide micelles, *Bull Korean chem. Soc.* 12 (1991) 411-413.
- [28] M. Ghiaci, R. Kia, R.J. Kalbasi, Investigation of thermodynamic parameters of cetylpyridinium bromide sorption onto ZSM-5 and natural clinoptilolite, *J. Chem. Thermodynamics* 36 (2004) 95-100.
- [29] S. Paria, K.C. Khilar, A review on experimental studies of surfactant adsorption at the hydrophilic solid-water interface, *Adv. Colloid Interface Sci.* 110 (2004) 75-95.
- [30] R. Atkin, V. S. J. Craig, S. Biggs, Adsorption kinetics and structural arrangements of cetylpyridinium bromide at the silica-aqueous interface, *Langmuir*, 17 (2001) 6155-6163.

Captions of figures and tables

Fig. 1. Effect of CP⁺ concentration on the turbidity of the electrolytic medium during EC in 0.1 M NaCl (aluminum electrodes; I = 0.2 A).

Fig. 2. Effect of CP⁺ concentration on the pH variation during EC in 0.1 M NaCl (aluminum electrodes; I = 0.2 A).

Fig. 3. Variation of CP⁺ concentration during EC in 0.1 M NaCl (aluminum electrodes; I = 0.2 A).

Fig. 4. Cyclic voltammograms of CP⁺ (glassy carbon electrode; scan rate of 100 mV/s; the increasing currents correspond to 0.6, 1.2, 2.4 and 3 mM CP⁺ in 0.1M NaCl solution).

Fig. 5. Scheme of the electrochemical behavior of CP⁺ in 0.1 M NaCl solution at a glassy carbon electrode.

Fig. 6. Effect of the cathode on the abatement of CP⁺ during EC in 0.1 M NaCl solution (aluminum anode; cathodes are specified in the figure; I = 0.2 A).

Fig. 7. Variation of pH during the phosphate-assisted EC (0.1 M NaCl buffered by 0.1 M Na₂HPO₄ + 0.1 M NaH₂PO₄; aluminum electrodes; I = 0.2 A).

Fig. 8. Variation of CP⁺ concentration during the phosphate-assisted EC (0.1 M NaCl buffered by 0.1 M Na₂HPO₄ + 0.1 M NaH₂PO₄; aluminum electrodes; I = 0.2 A).

Fig. 9. Adsorption kinetics of CP⁺ onto (a1) (AlPO₄)_C (b1) (AlPO₄)_E and adsorption isotherm onto (a2) (AlPO₄)_C (b2) (AlPO₄)_E at 22°C and pH 7.9

Fig. 10. Adsorption kinetic (a) and isotherm adsorption (b) of CP⁺ onto alumina modified by adsorbed phosphate at 22°C and pH 6.9.

Table 1. Second-order kinetic parameters for the removal of CP⁺ by (AlPO₄)_E and (AlPO₄)_C at different initial concentrations of CP⁺.

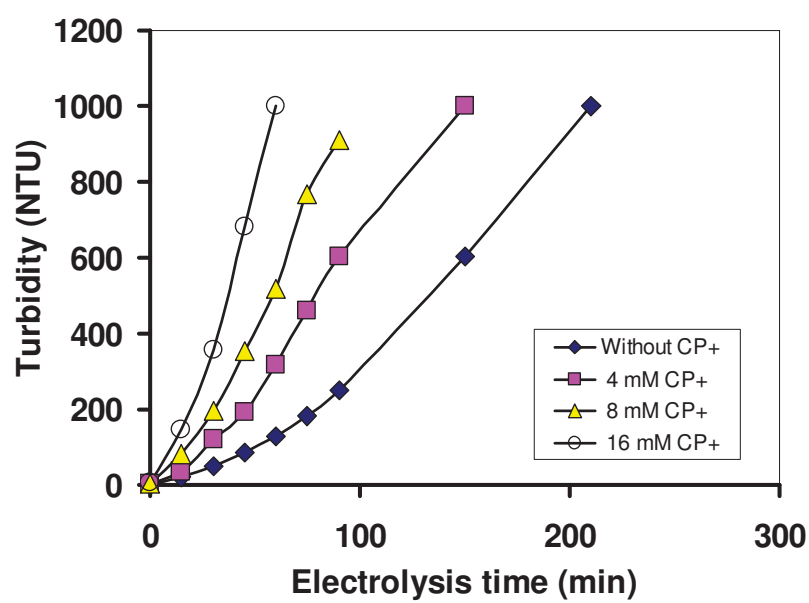


Fig. 1.

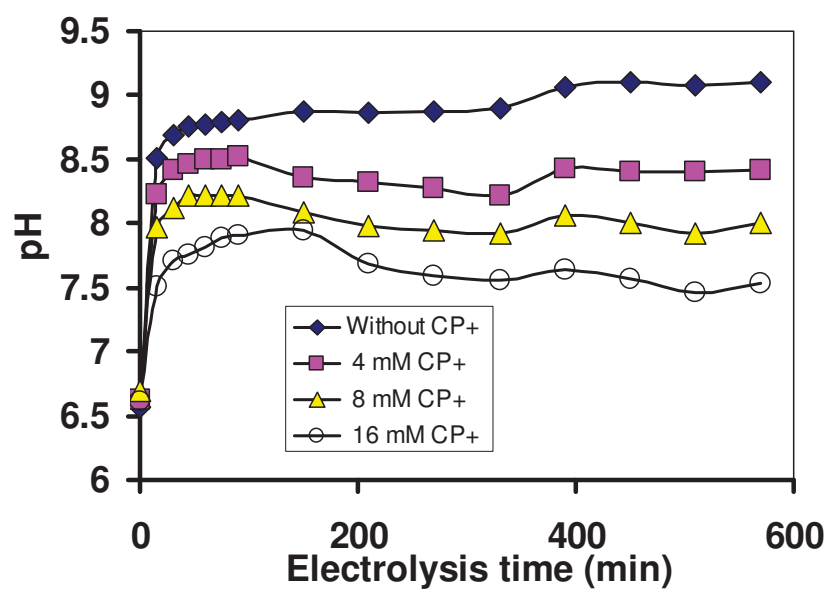


Fig. 2.

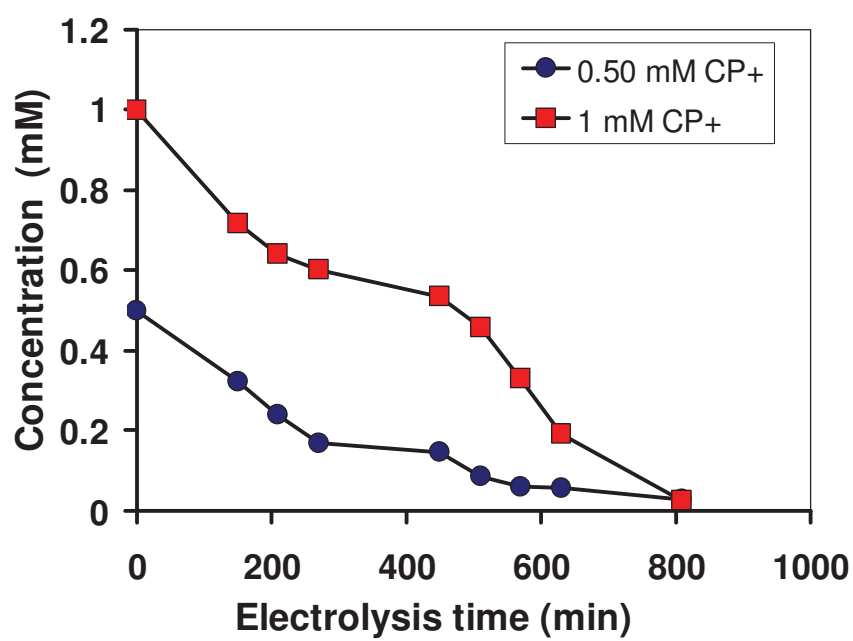


Fig. 3.

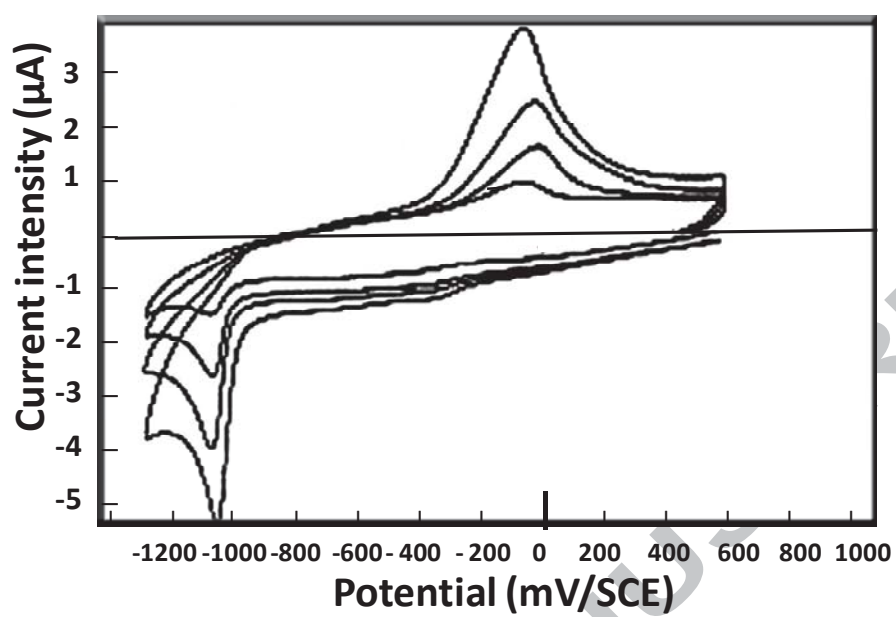


Fig. 4.

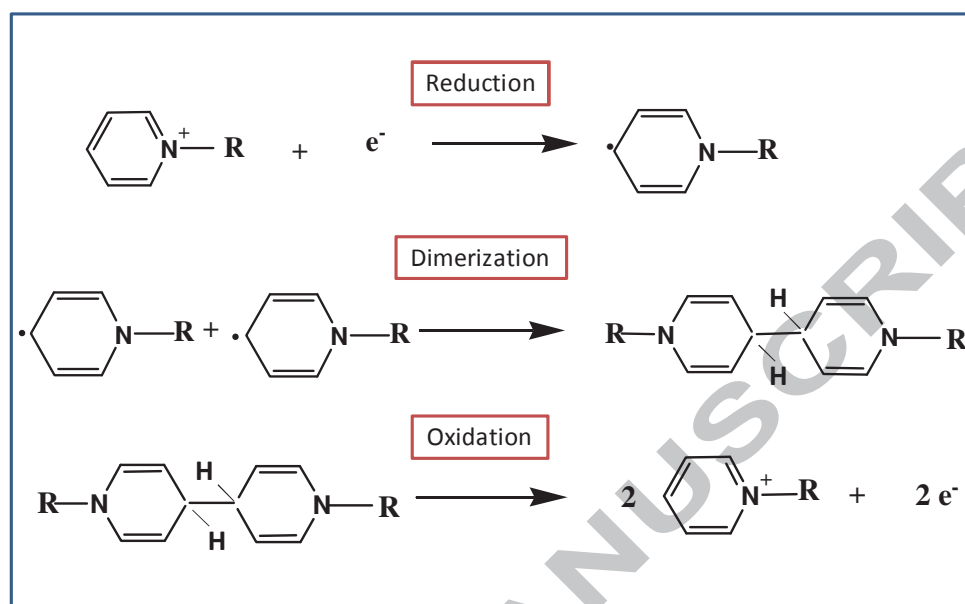


Fig. 5.

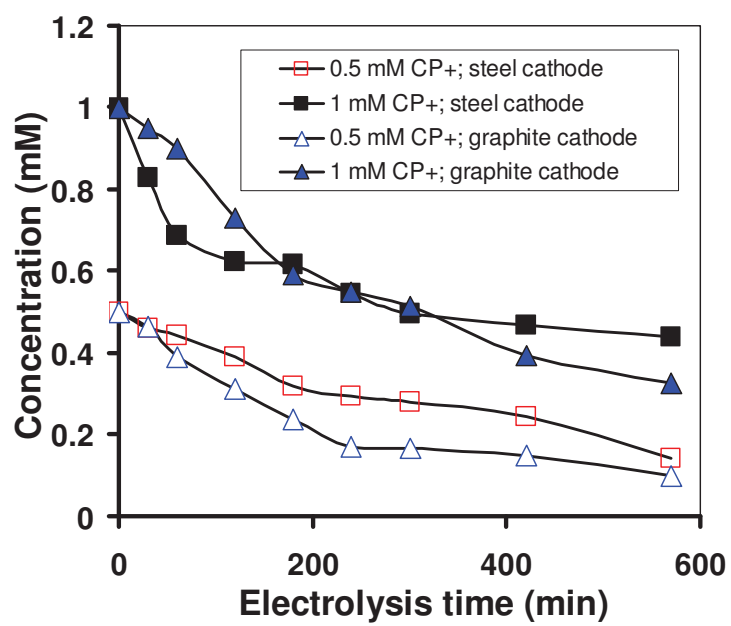


Fig. 6.

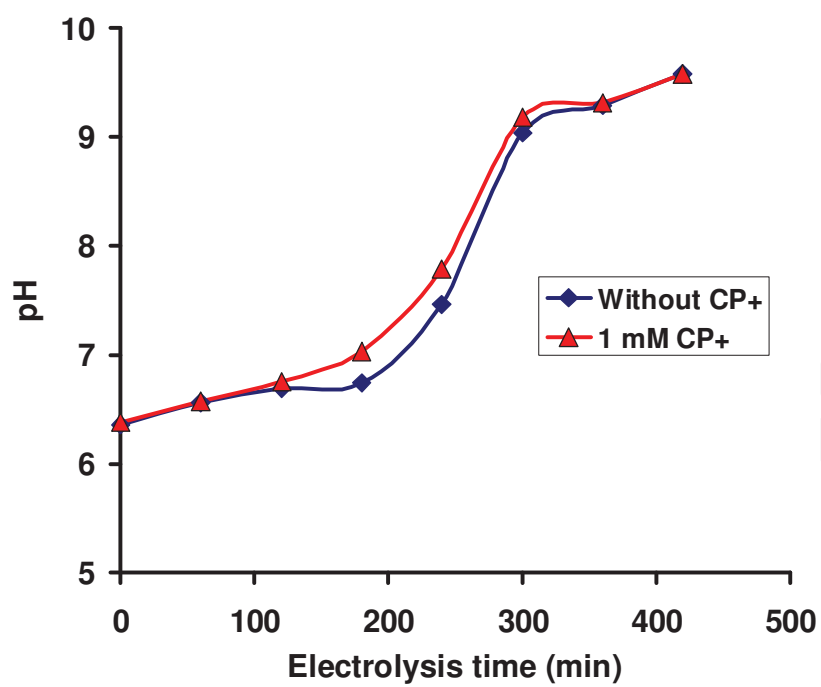


Fig. 7.

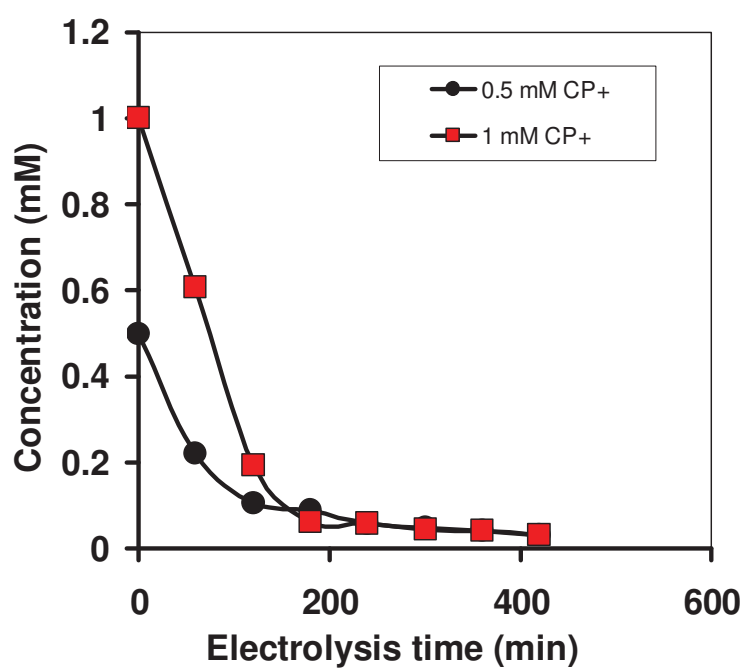


Fig. 8.

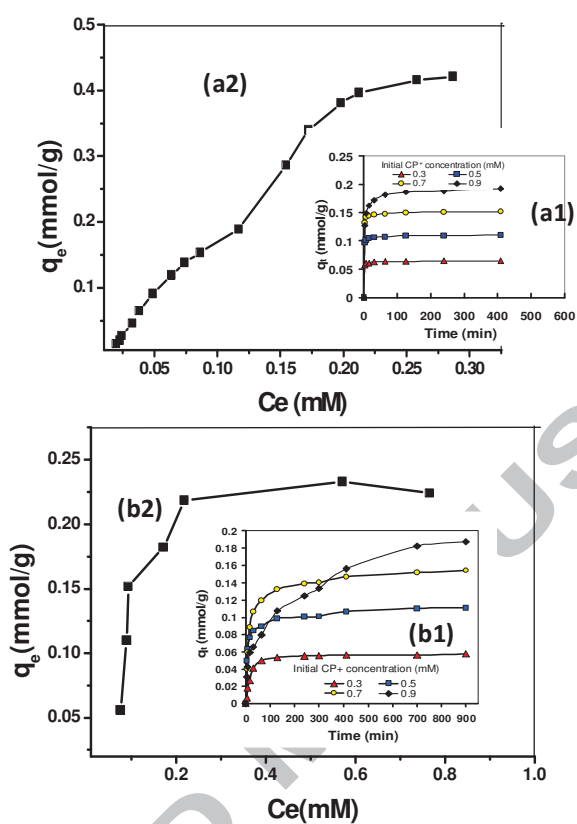


Fig. 9. Adsorption kinetics of CP⁺ onto (a1) (AlPO₄)_C (b1) (AlPO₄)_E and adsorption isotherm onto (a2) (AlPO₄)_C (b2) (AlPO₄)_E at 22°C and pH 6.9

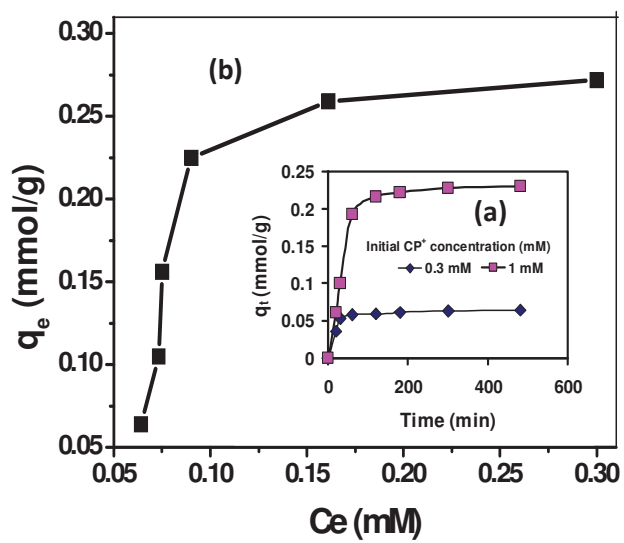


Fig. 10. Adsorption kinetic (a) and isotherm adsorption (b) of CP^+ onto alumina modified by adsorbed phosphate at 22°C and pH 6.9.

Revised table with all modifications

Table 1. Second order kinetic parameters for the removal of CP⁺ by (AlPO₄)_E and (AlPO₄)_C at different initial concentrations of CP⁺.

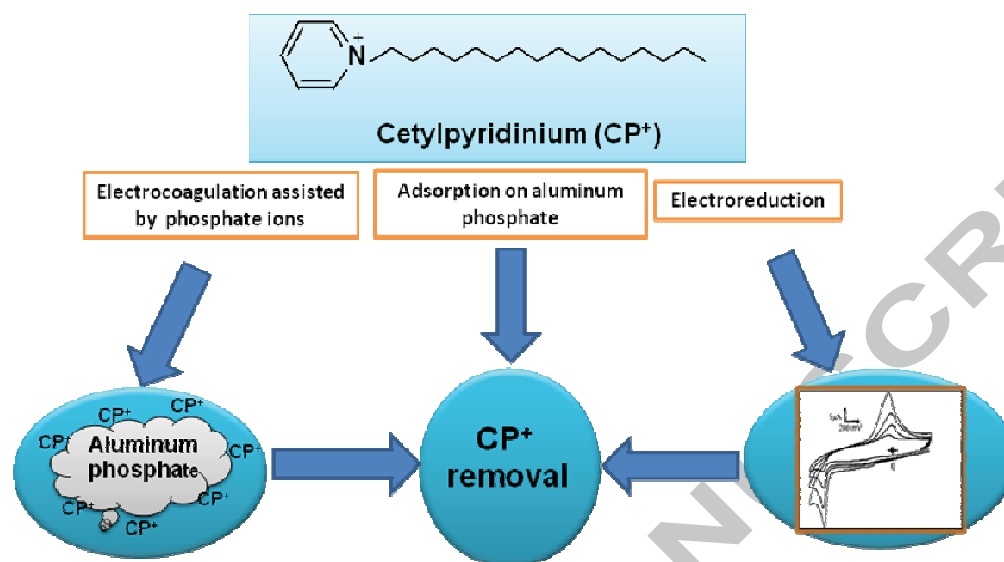
Adsorbent	Initial concentration of CP ⁺ (mM)	Pseudo second order model			
		q _e (exp) (mmol/g)	q _e (calc) (mmol/g)	k ₂ (g/mmol min)	R ²
(AlPO ₄) _E	0.3	0.0465	0.0580	0.9205	0.9994
	0.5	0.1000	0.1112	0.6370	0.9991
	0.7	0.1410	0.1554	0.3604	0.9994
	0.9	0.1810	0.1949	0.0693	0.9804
(AlPO ₄) _C	0.3	0.0515	0.0647	16.63	1
	0.5	0.1105	0.1103	7.499	1
	0.7	0.1540	0.1520	4.947	1
	0.9	0.1870	0.1925	1.555	0.999

Revised table

Table 1. Second order kinetic parameters for the removal of CP⁺ by (AlPO₄)_E and (AlPO₄)_C at different initial concentrations of CP⁺.

Adsorbent	Initial concentration of CP ⁺ (mM)	Pseudo second order model			
		q _e (exp) (mmol/g)	q _e (calc) (mmol/g)	k ₂ (g/mmol min)	R ²
(AlPO ₄) _E	0.3	0.0465	0.0580	0.9205	0.9994
	0.5	0.1000	0.1112	0.6370	0.9991
	0.7	0.1410	0.1554	0.3604	0.9994
	0.9	0.1810	0.1949	0.0693	0.9804
(AlPO ₄) _C	0.3	0.0515	0.0647	16.63	1
	0.5	0.1105	0.1103	7.499	1
	0.7	0.1540	0.1520	4.947	1
	0.9	0.1870	0.1925	1.555	0.999

Graphical abstract



Highlights

The electrocoagulation treatment of cetylpyridinium (CP⁺) was investigated.

CP⁺ abatement involved adsorption and electroreduction.

More efficient CP⁺ removal was observed in the presence of phosphate ions.

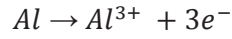
Alumina modified by adsorbed phosphate improves the CP⁺ adsorption.

ACCEPTED MANUSCRIPT

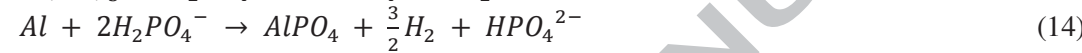
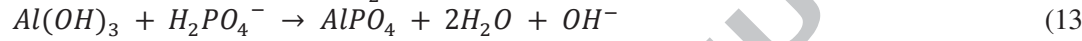
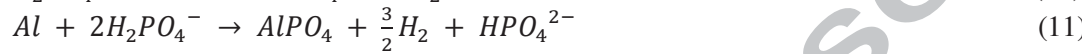
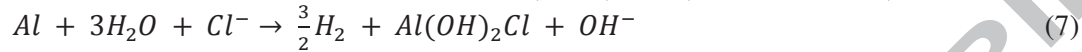
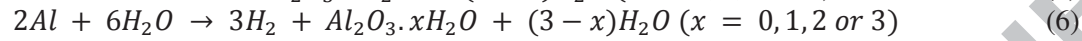
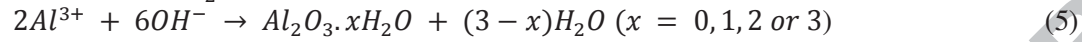
$$q_t = \frac{(C_0 - C_t)V}{m} \quad (1)$$

$$q_t = \frac{(C_0 - C_e)V}{m}$$

(2)



(3)



$$\log(q_e - q_t) = \log q_e - \frac{k_1 t}{2.303} \quad (15)$$

$$\frac{t}{q_t} = \frac{1}{k_2 q_e^2} + \frac{t}{q_e}$$

(16)